POLITECNICO DI TORINO
Repository ISTITUZIONALE

ESDN inhibits melanoma progression by blocking E-selectin expression in endothelial cells via STAT3

Original
ESDN inhibits melanoma progression by blocking E-selectin expression in endothelial cells via STAT3 / Coppo, R., Orso, F., Virga, F., Dalmasso, A., Baruffaldi, D., Nie, L., Clapero, F., Dettori, D., Quirico, L., Grassi, E., Defilippi, P., Provero, P., Valdembri, D., Serini, G., Sadeghi, M.M., Mazzone, M., Taverna, D.. - In: CANCER LETTERS. - ISSN 0304-3835. - ELETTRONICO. - 510:(2021), pp. 13-23. [10.1016/j.canlet.2021.04.005]

Availability:
This version is available at: 11583/2928112 since: 2021-09-29T15:36:49Z

Publisher:
Elsevier

Published
DOI:10.1016/j.canlet.2021.04.005

Terms of use:

This article is made available under terms and conditions as specified in the corresponding bibliographic description in the repository

Publisher copyright

(Article begins on next page)

17 October 2026

Predicting the consequences of a NaTech event: occupational short-term inhalation risk supported by advanced pollutant dispersion modelling.

Marco Ravina[1], Marta Brignone[1], Federico Urbinati[1], Claudia Schiavini[1 2], Mariachiara Zanetti[1], Deborah Panepinto[1]

[1] Department of Environment, Land and Infrastructure Engineering, Politecnico di Torino, Corso Duca degli Abruzzi 24, 10129 Torino, Italy

[2] Ecole Centrale de Lyon, CNRS, Universite Claude Bernard Lyon 1, INSA Lyon, LMFA, UMR5509, 69130, Ecully, France

Corresponding author: Marco Ravina, Department of Environment, Land and Infrastructure Engineering, Politecnico di Torino, Corso Duca degli Abruzzi 24, 10129 Torino, Italy, marco.ravina@polito.it

EDITOR'S NOTE: This article is part of the special series "RemTech Europe 2024: Comprehensive Approaches for the Management of Contaminated Sites." The series collects new frontiers to fighting and managing "old" and "new" contaminants that can be found in environmental sites.

Acknowledgement

This study was carried out within the framework of the RETURN Extended Partnership that received European Union funding Next-GenerationEU (National Recovery and Resilience Plan - NRRP, Mission 4, Component 2, Investment 1.3 - D.D. 1243 2/8/2022, PE00005) - SPOKE TS 2

© The Author(s) 2025. Published by Oxford University Press on behalf of the Society of Environmental Toxicology and Chemistry. All rights reserved. For permissions, please email: journals.permissions@oup.com.

Downloaded from https://academic.oup.com/ieam/advance-article/doi/10.1093/inteam/vjaf073/8164122 by guest on 27 June 2025

Data Availability statement

Data are available upon request from corresponding author Marco Ravina (marco.ravina@polito.it).

Author contributions

Conceptualization: M.R., D.P., M.Z.; Data curation: M.R., C.S., D.P.; Formal analysis: M.R., D.P., M.Z.; Funding acquisition: D.P., M.Z.; Investigation: M.R., M.B., F.U., C.S., D.P.; Methodology: M.R., D.P.; Project administration: D.P., M.Z.; Resources: M.R., D.P., M.Z.; Software: M.R., M.B., F.U., C.S.; Supervision: M.R., D.P., M.Z.; Validation: M.R., D.P., M.Z.; Visualization: M.R., M.B., D.P., M.Z.; Writing – original draft: M.R., M.B., F.U., D.P.; Writing – review and editing: M.R., M.B., D.P., M.Z.

Downloaded from https://academic.oup.com/ieam/advance-article/doi/10.1093/inteam/vjaf073/8164122 by guest on 27 June 2025

Predicting the consequences of a NaTech event: occupational short-term inhalation risk supported by advanced pollutant dispersion modelling.

ABSTRACT

In this work, a methodology for the preventive assessment of the risk associated with the accidental inhalation of toxic substances at an industrial site is presented. The methodology is based on a NaTech (Natural-Hazard Triggered Technological Accidents) sequence modelling: event and site characterisation; simulation of the accidental release and pollutant dispersion; and calculation of short-term risk, by averaging concentrations and comparing them with the reference values proposed by the main occupational exposure organizations worldwide. The proposed model is applied to a case study of a chemical company in central Italy. A hypothetical vessel failure leads to a pool release, evaporation, and dispersion of tetrahydrofuran. A pool evaporation model is applied, and the Lagrangian particle model Parallel Micro-Swift Spray (PMSS) is used for dispersion modelling. The resulting concentration fields show that the pollutant magnitude and distribution can vary depending on wind speed and direction and atmospheric conditions. Concentrations decrease rapidly with distance from the source, both horizontally and vertically. The maximum modelled concentration of 596 mg m^{-3} is recorded at the emission source. Inhalation hazard quotient (HQ) is calculated against the threshold limit value - Short Term Exposure Limit (TLV-STEL = 295 mg m^{-3}). HQ exceedances are reported at the emission source. No exceeding is reported away from the source. The uncertainty on the calculated risk arises from considerations on modelling choices, threshold limit values, and the correction method for short-term concentration averaging. For the proposed general methodology, the presented model can be applied with relatively limited calculation resources and practical applicability.

Downloaded from https://academic.oup.com/ieam/advance-article/doi/10.1093/inteam/vjaf073/8164122 by guest on 27 June 2025

KEYWORDS: hazardous pollutants; inhalation risk; pollutant dispersion; industrial accidents; health risk

INTRODUCTION

Natural disasters can have devastating effects on industrial infrastructure, leading to technological accidents commonly referred to as NaTech events (Natural-Hazard Triggered Technological Accidents). These events arise from the interplay between natural phenomena, such as earthquakes, floods, and hurricanes, and technological incidents involving the release of hazardous substances (Cruz & Suarez-Paba, 2019). The impact of NaTech events is particularly significant in industrial settings where dangerous materials are present, potentially resulting in accidental spills and the subsequent dispersion of pollutants that pose serious risks to human health and the environment. In Europe, the Seveso-III Directive (Directive 2012/18/EU; European Commission, 2024) on the control of major-accident hazards involving dangerous substances depicts the necessary framework for risk management strategies aimed at preventing serious accidents and minimizing their effects. Depending on the quantity of hazardous materials present, different safety regulations apply to different sectors.

Historically, several significant NaTech incidents have underscored the need for improved risk assessment and management strategies. Major accidents that have occurred on EU territory are detailed in the MINERVA database (European Commission, 2024a). The European Commission Joint Research Centre's Major Accident Hazards Bureau developed this portal with the intention of giving users access to all available data on ongoing operations, pertinent

Downloaded from https://academic.oup.com/ieam/advance-article/doi/10.1093/inteam/vjaf073/8164122 by guest on 27 June 2025

publications, and resources for managing significant chemical dangers (Cangmin and Klauk, 2020).

The assessment of risks associated with NaTech events involves several challenges, primarily due to the unpredictable nature of natural hazards and their cascading effects on industrial operations. Natural hazards can cause rapid changes in environmental conditions, leading to sudden releases of hazardous substances. Assessing the dispersion and impact of such releases thus requires models that can handle high temporal and spatial variability (Blocken et al., 2008). One of the most critical aspects of a NaTech event is the inhalation risk posed to workers by toxic substances (Shafiei Moghaddam et al., 2023). Incidents that involve the release of volatile chemicals can expose personnel to hazardous concentrations of pollutants within very short time frames. Therefore, timely and accurate assessment of inhalation risk is essential for protecting worker health and for emergency planning. Yet traditional methods for inhalation risk assessment often fall short of providing the precise evaluations needed in the dynamic and complex scenarios typical of NaTech events (Krausmann et al., 2017). Traditional approaches may not adequately account for the intricate and variable dynamics of airborne pollutant dispersion or the fluctuating environmental and operational conditions at industrial sites. However, recent advancements in computational modelling have significantly improved the ability to predict pollutant dispersion in complex scenarios (Dou et al., 2022). High-resolution models, such as Computational Fluid Dynamics (CFD) models and Lagrangian particle dispersion models, offer detailed insights into the behaviour of pollutants in various environmental conditions. These models consider factors such as wind speed and direction, temperature, topography, and building structures, to accurately simulate the dispersion patterns of hazardous substances.

Downloaded from https://academic.oup.com/ieam/advance-article/doi/10.1093/inteam/vjaf073/8164122 by guest on 27 June 2025

Several studies have been published on the prediction of acute health risks consequent to rapid and unexpected pollutant releases. All these studies have involved the integration of dispersion and transport modelling with risk analysis. Hassan Bhat et al. (2021) carried out a review describing different approaches for air pollution health risk assessment. The reported studies differed in the scale of analysis or the applied tools. The majority of such studies have been based on a local or regional scale—i.e., 10-100 km of domain extension (Malakan et al., 2024; Karaca et al., 2021; Jones et al., 2023). Regarding modelling tools, AERMOD (Teggi et al., 2018; Malakan et al., 2024), CALPUFF (Jones et al., 2023), HYSPLIT (Karaca et al., 2021), and a modified Lagrangian model (Kocijan et al., 2023) have been used. Fewer studies have focused on microscale dispersion (0.1 – 1 km of domain extension) and risk characterisation. To the authors' knowledge, none have been related to tetrahydrofuran.

Recent advancements in computational power and data availability have significantly enhanced the capabilities of high-resolution dispersion models. However, several challenges remain. One major issue is the uncertainty associated with model inputs, such as emission rates, meteorological data, and exposure definition. At the microscale, following an accidental release, the concentration of hazardous substance can reach high levels, especially in areas close to the emission source. Downscale modelling is thus usually required to take into account the effects of the terrain and buildings (Zhang & Wang, 2022). In previous research, the impact of buildings on the spatial extension of hazardous concentration has been found to be noteworthy (Rademaeker & Associazione Italiana di Ingegneria Chimica, 2012). For all the above reasons, there is a need for a better integration of high-resolution pollutant dispersion models with advanced short-term inhalation risk modelling techniques.

This study aims to address current research gaps in the field, in order to obtain a realistic simulation of accidents within a reasonable timeframe in the case of complex study domains,

Downloaded from https://academic.oup.com/ieam/advance-article/doi/10.1093/inteam/vjaf073/8164122 by guest on 27 June 2025

characterised by constructed elements that interfere with the dispersion of released substances. The innovative elements of this study are found in particular in the choice of the type of model used (a microscale Lagrangian model based on the parameterization of atmospheric variables), and the integration of dispersion calculation with risk analysis, through the calculation of a concentration value which is representative of the acute exposure period.

The objective of this work is thus to propose an integrated methodology for the preventive assessment of the risk associated with the inhalation of a toxic substance (tetrahydrofuran) at an industrial site, by workers, following an accidental spill and release caused by a NaTech event. This study integrates predictive modelling and spatial mapping to enhance the response and planning capacity of local authorities and communities. The aim is to promote a more proactive and responsible management of technological risks, especially in the context of climate change. The methodology is based on a first phase in which the event typology and the industrial site (built elements, hazardous substances, meteorology etc.) are characterised. Subsequently, the possible accidental releases are modelled, and the dispersion of the toxic substances into the surroundings of the source and around the production site is simulated. Finally, exposure levels can be combined with toxicological data to estimate the potential health risks associated with the inhalation of the released substances. An innovative element provided by the model is that it can estimate the risk considering any inhalation period, even on timesteps smaller than the simulation timestep. To simulate the toxic dispersion, models taking into account the possible presence of obstacles and constructed elements in the surroundings of the emission source are considered. A short-term risk characterisation is conducted by comparing the concentrations obtained with the reference concentrations proposed by the main worldwide occupational exposure organizations. By providing timely

Downloaded from https://academic.oup.com/ieam/advance-article/doi/10.1093/inteam/vjaf073/8164122 by guest on 27 June 2025

and accurate estimates of pollutant concentrations, the proposed approach can enhance emergency management strategies and worker health protection practices. The proposed model was applied to a hypothetical preventive case study, corresponding to a chemical company located in central Italy.

METHODOLOGY

Approach description

The workflow of the proposed methodology is presented in Figure 1. The approach involves four phases: a first phase in which, following the triggering accident, the event typology, source and substance involved are characterised; a second phase in which the accidental release is modelled; a third phase in which the dispersion of the toxic substance into the surroundings of the source and around the production site is simulated; and a fourth phase in which exposure levels are combined with toxicological data to estimate the health risks associated with inhalation of the released substances. To demonstrate the effectiveness of the proposed methodology, a case study application is presented. The case study involves a hypothetical NaTech event at a chemical manufacturing facility, triggered by flooding. The event leads to the release of tetrahydrofuran, a volatile organic compound highly toxic to human health, from a storage tank, with subsequent dispersion across the site.

Hazardous material characterisation

The amount and type of hazardous materials handled at the facility determine the degree of risk. The substance could be chemical materials meant to be used in the manufacturing of agricultural products (fertilizers, etc.) or pharmaceutical products, or it could be petrochemicals such as tar or gasoline. Possible sources of data regarding substance toxicity are provided by the American Conference of Governmental Industrial Hygienists (ACGIH;

Downloaded from https://academic.oup.com/ieam/advance-article/doi/10.1093/inteam/vjaf073/8164122 by guest on 27 June 2025

American Conference of Governmental Industrial Hygienists, 2024), the National Institute for Occupational Safety and Health (NIOSH; National Institute for Occupational Safety and Health, 2024), the Occupational Safety and Health Administration (OSHA; Occupational Safety and Health Administration, 2024), the European Commission Scientific Committee on Occupational Exposure Limits (SCOEL; European Commission, 2024a), SafeWork Australia (SafeWork Australia, 2024), and the UK Control of Substances Hazardous to Health (COSHH; United Kingdom Government, 2024).

Material release

In the release phase of modelling, the source term is defined. The amount and physical characteristics of the emitted hazardous material, such as temperature, pressure, release duration, and substance state, are included in this characterisation (Fabbri & Wood, 2019). The status and characteristics of the released material (such as compressed gas, liquefied-pressurized gas, non-boiling liquid, etc.), as well as the damage processes (such as vessel rupture, hole failure) are intimately associated with the source term (Fabbri & Wood, 2019). While pressurized liquid releases are complicated and involve a two-phase flow, compressed vapor releases often occur in the gaseous phase (European Commission Joint Research Centre, 2017). Following the release, the pressure decreases to the ambient level (Houf & Winters, 2013). Following dilution, the buoyancy is low when the density of the expelled plume approaches that of the ambient environment. Stable stratification brought on by density may inhibit vertical turbulence mixing for substances with a higher density, making it more difficult for the ambient turbulence to reach the dense gas plume and thus preventing the plume from dissipating (Zhang and Wang, 2022). Moreover, the substance may be subject to gravity-driven flow, causing it to follow the topography rather than the ambient wind. In the release

Downloaded from https://academic.oup.com/ieam/advance-article/doi/10.1093/inteam/vjaf073/8164122 by guest on 27 June 2025

model of densely liquefied gases, temperature is therefore a crucial parameter (Koopman & Ermak, 2007).

Atmospheric dispersion

After the release, the atmospheric transport of hazardous substances is influenced by turbulence scale. At the microscale, near the source, thorough characterisation of the turbulence structure is necessary for a proper evaluation of the transport. Advection and diffusion are the main processes involved in the atmospheric transport of hazardous pollutants, and they are influenced by a variety of climatic factors such as wind direction, atmospheric stability, height of the atmospheric boundary layer, and precipitation. Various methods, including Gaussian plume, Lagrangian puff and particle, chemical transport models (Zhang & Wang, 2022), and computational fluid dynamics (CFD), have been developed to simulate the atmospheric dispersion of hazardous pollutants. In most cases, downscale modelling is necessary to account for the effects of infrastructure and terrain. Applications include the GRAMM-GRAL model (Berchet et al., 2017), the Parallel Micro-Swift Spray (PMSS) model (Oldrini et al., 2017), the Simulator fOr Wind Farm Applications (SOWFA) (Fleming et al., 2017), and the Quick Urban & Industrial Complex (QUIC) Dispersion Modeling System (Gowardhan et al., 2011). The use of a Lagrangian particle model seems a good trade-off between the need for efficient computational cost versus accounting obstacles (Trini Castelli et al., 2018). More details about these models can be found in any systematic review study (e.g. Markiewicz, 2012).

Another crucial aspect in preventive consequential analysis is the selection of meteorological and atmospheric data on which the simulation of the accident is based. Such data must reflect the most critical conditions with respect to pollutant dispersion—the ideal ones being a stable atmosphere and low wind velocity. Two different approaches can be

Downloaded from https://academic.oup.com/ieam/advance-article/doi/10.1093/inteam/vjaf073/8164122 by guest on 27 June 2025

adopted in this phase: using and elaborating existing datasets, or generating synthetic time series. Because meteorological conditions are typically uniform within the horizontal scale, meteorological observations from a monitoring site can be used to estimate atmospheric dispersion in the first scenario, provided the simulation is based on available data and the horizontal scale is constrained (Zhang and Wang, 2022).

Meteorological and geophysical data of the domain can be processed by means of dedicated models, which provide characteristic parameters describing atmospheric conditions. The most important is the Monin-Obukhov length (L_M), a fundamental parameter in micrometeorology, used to describe conditions of atmospheric stability or instability within the boundary layer (Monin and Obukhov, 1954). The Monin-Obukhov length indicates the vertical distance above the Earth's surface at which heat and momentum fluxes have equivalent effects on turbulence production. Atmospheric stability conditions can be derived based on the sign and value of L_M,. In the second case (generation of synthetic dispersion parameters), a number of different methods have been proposed, although it is difficult to make precise predictions about local wind direction, speed, and atmospheric stability. The most widely used methods for forecasting future winds and other meteorological parameters with ever-increasing spatial and temporal resolution are numerical weather prediction (NWP) models (Perne et al., 2021; Grašič et al., 2018). Alternative methods for obtaining local wind signal values at the site of a portable meteorological station have been proposed based on artificial neural networks (Torrontegui & García-Ripoll, 2019), fuzzy models (Pal et al., 2018), and Volterra models (Carini et al., 2018).

Risk characterisation

In the standard approach for short-term toxicity assessments, risk R can be evaluated by calculating hazard quotients (HQ) for individual contaminants. A hazard quotient is the ratio

Downloaded from https://academic.oup.com/ieam/advance-article/doi/10.1093/inteam/vjaf073/8164122 by guest on 27 June 2025

212 of the exposure concentration (EPC) to a reference concentration (RfC), multiplied by an
213 exposure factor EF (Equation 1; U.S. Environmental Protection Agency, 2024b).

214 $$R = \frac{EPC}{RfC} EF \qquad (1)$$

215 The inhalation RfC is the concentration of a pollutant in air, that is unlikely to cause toxic
216 harmful effects for the specified duration of exposure. The RfC selected must be appropriate
217 for the exposure duration. If the HQ calculated is equal to or less than 1, toxic adverse health
218 effects are not expected to result from exposure to the pollutant (Ravina, Facelli, et al., 2020).

219 Occupational exposure limits are mostly defined for full shift (8-hour) exposure because of
220 concerns about the long-term health impacts of exposure to airborne contaminants. A full
221 shift exposure level can be utilized to determine acute exposure estimates (Maidment, 1998).
222 The fact that most exposure distributions tend to be lognormal and that the geometric mean
223 (GM) and geometric standard deviation (GSD) of such distributions with varying averaging
224 periods are related serves as the foundation for extrapolating full shift exposure estimates to
225 acute ones (National Institute for Health, 1994). For the assessment of the impact caused by
226 toxic pollutants, the average concentration over short time intervals, on the order of minutes,
227 should be used. However, since most legislation and some dispersion models deal with hourly
228 average concentrations, a method for deriving short-term mean from hourly mean must be
229 applied. Several alternative techniques have been developed and presented. The most widely
230 used techniques designed to overcome this limitation are those calculating the peak-to-mean
231 ratio or factor and using the power law function (Melo et al., 2023). Peak-to-mean factors are
232 extensively applied to odour dispersion problems (Ravina, Bruzzese, et al., 2020). Brancher et
233 al. (2020) compared three alternative formulations of the peak-to-mean approach: a constant
234 factor of 4, an empirically based peak-to-mean procedure, and a concentration-variance

Downloaded from https://academic.oup.com/ieam/advance-article/doi/10.1093/inteam/vjaf073/8164122 by guest on 27 June 2025

computation. This last has shown better consistency with experimental measurements, although with higher applicative complexity. A simple and relatively consolidated approach involves the use of a power law function, according to:

$$\frac{\overline{C}(\Delta\tau)}{\overline{C}(\Delta T)} = \left(\frac{\Delta T}{\Delta\tau}\right)^n \qquad (2)$$

where $\overline{C}(\Delta\tau)$ is the average concentration over the resolution time $\Delta\tau$ (seconds or minutes), and $\overline{C}(\Delta T)$ is the average concentration over a longer time ΔT (typically one hour). The value of the exponent *n* for mean times of 1 hour or less appears to be mainly influenced by the height of the source and by atmospheric stability. The n values derived from field data show a range of 0.2-0.5 for ground-level sources and 0.12-0.7 for elevated sources (Bartzis et al., 2008).

Case study

A chemical production industry located in central Italy was selected as a case study. The accident proposed in the study aims at preventively assessing the possible dynamics of a real NaTech reported in the database on an existing industrial site. Given the available data, the dynamics of the accident (sequence and typology) were reproduced from an original event, while the site of occurrence and meteorology were chosen arbitrarily. The industrial complex covers an area of approximately 145,000 m^2. It is primarily oriented in the northwest/southeast direction, with an approximate extension of 450 metres. The buildings within the complex house production facilities, including several tanks containing solvents with varying levels of hazard. The structure is located 20 km from the sea, on predominantly flat terrain (Figure 2).

To simulate the dynamics of the triggering event, the eMARS (Major Accident Reporting System) database (European Commission, 2024b) was used. The eMARS database collects

Downloaded from https://academic.oup.com/ieam/advance-article/doi/10.1093/inteam/vjaf073/8164122 by guest on 27 June 2025

information on accidents and accident-free situations in the European Union through a mixed mandatory and voluntary reporting system. The records provide detailed descriptions of accidents, including information on the facility and substances involved, along with the causes, consequences and response procedures. The triggering natural event occurred on August 15, 2002. As a secondary consequence of the flooding event, an ethylbenzene storage tank was seriously damaged. Solvent leakage subsequently occurred, resulting in the solvent's release into the atmosphere. In this study, ethylbenzene was replaced with tetrahydrofuran, to evaluate the consequences of the release of a highly volatile and toxic substance.

The storage tank damaged by the NaTech event has a cylindrical geometry (diameter 15 m, height 9 m). It is placed within a containment basin of square footprint (height 2 m, side length 30 m). The tank was filled to 80% capacity with tetrahydrofuran (Figure 2).

Tetrahydrofuran, also known as oxolane, is a cyclic ether that contains one oxygen and four carbon atoms. It functions as a solvent that is polar and aprotic. It belongs to the family of volatile organic compounds, cyclic ethers, saturated organic heteromonocyclic parents, and oxolanes. It is a low-viscosity, colourless, organic liquid that dissolves in water. Its primary application is as a precursor to polymers. Tetrahydrofuran is a multipurpose solvent since it is polar and has a broad liquid range. The main properties of tetrahydrofuran are reported in Table 1. Exposure to tetrahydrofuran can cause a number of different symptoms depending on the route of exposure. In case of inhalation, symptoms include coughing, a burning sensation in the throat and chest, dizziness, headache, nausea and loss of consciousness. Prevention involves the use of ventilation, localized suction or respiratory protective equipment (Dannan, 2015).

Release model and evaporation model

Downloaded from https://academic.oup.com/ieam/advance-article/doi/10.1093/inteam/vjaf073/8164122 by guest on 27 June 2025

In the case study, the release of tetrahydrofuran in a liquid state and subsequent evaporation was simulated. The tank was not under pressure. The release occurred at the bottom of the tank, in correspondence of the rupture of an emptying pipe of 100-mm diameter. The solvent spilled into the containment basin, forming a pool that evaporated and dispersed into the surroundings. It was assumed that the containment basin was empty at the time of release, and therefore not directly affected by the meteorological phenomenon (i.e. no solvent dilution due to the presence of water). For the modelling of release dynamics, the approach proposed by (van den Bosch, 2005) was applied. MathWorks Matlab® (Mathworks Inc., 2024) was used as the modelling tool.

The mass flow rate of a discharge is governed by hydraulic pressure, which depends on the liquid level in the tank. The model was based on mass balance solving, adopting an iterative numerical procedure. The initial liquid volume and mass were calculated as:

$$Q_{L,1} = \varphi * \mathrm{V} * \rho_L \qquad (3)$$

$$V_{L,1} = Q_{L,1}/\rho_L \qquad (4)$$

where $Q_{L,1}$ is the initial mass of liquid contained in the vessel [kg], φ is the filling degree [m^3 m^{-3}], V is the vessel volume [m^3], and ρ_L is the liquid density [kg/m^3]. The Bernoulli's equation was employed for calculating the mass flow rate, neglecting the initial velocity of the liquid in the container:

$$q_s = C_d * A_h * \sqrt{(2(P - P_a) * \rho_L} \qquad (5)$$

$$P = P_h + P_{aL} \qquad (6)$$

$$P_h = \rho_L * g * h_L \qquad (7)$$

Downloaded from https://academic.oup.com/ieam/advance-article/doi/10.1093/inteam/vjaf073/8164122 by guest on 27 June 2025

where A_h is the cross-sectional area of the hole [m^2], C_d is the discharge coefficient [-], g is the gravitational acceleration [m s^{-2}], h_L is the liquid height (relative to the vessel base) [m], P is the total pressure at the opening [N m^{-2}], P_h is the (hydraulic) liquid pressure [N m^{-2}], P_{aL} is the external pressure above liquid [N m^{-2}], Pa is the atmospheric pressure [N m^{-2}], and q_s is the mass flow rate [kg s^{-1}]. A time step δt was defined by freely choosing N_t, and for each time step, the differential mass released δQ was calculated:

$$\delta t = t_{end}/N_t \qquad (8)$$

$$\delta Q = -q_{s,i} * \delta t \qquad (9)$$

The liquid content decrease was calculated as:

$$\delta V_L = \frac{\delta Q}{\rho_L} \qquad (10)$$

Thus, obtaining the liquid volume at the time step i+1:

$$V_{L,i+1} = V_{L,i} + \delta V_L \qquad (11)$$

Based on the tank geometry, the new liquid level inside the tank was calculated:

$$\delta h_L = \delta V_L / A_{L,i} \qquad (12)$$

$$h_{L,i+1} = h_{L,i} + \delta h_L \qquad (13)$$

where $A_{L,i}$ is the tank area. Iteration stopped when the liquid height was lower than the hole height.

In conjunction with the tank emptying process, code was implemented to simulate the evaporation of the solvent mass that accumulated in the containment basin. The evaporation of the liquid was assumed to start simultaneously with the liquid's settling in

Downloaded from https://academic.oup.com/ieam/advance-article/doi/10.1093/inteam/vjaf073/8164122 by guest on 27 June 2025

the containment basin. Consequently, the mass of the pool at each time step i was replenished by the mass of liquid released from the tank at the time step i-1:

$$M_{pool,i} = M_{pool,i-1} + M_{released,i-1} - M_{evaporated,i-1} \quad (14)$$

It was assumed that the liquid instantly covered the entire surface of the collection basin.

The mass flow rate of evaporation $q_v^{''}$ was calculated using the mean of the mass transfer coefficient and the vapor concentration at the liquid surface of the basin.

$$q_v^{''} = k_m * c_i \quad (15)$$

where c_i is the concentration component i [kg m^{-3}], $k_m$is the mass transfer coefficient [m s^{-1}], and $q_v^{''}$ is the vaporisation mass flux [kg m^{-2}·s^{-1})]. The mass transfer coefficient k_m was calculated with the model proposed by Kawamura and Mackay (1987):

$$k_m = C_{m\&m} * u_{w,10}^{0.78} * \left(2 * r_p\right)^{-0.11} * Sc^{-0.67} \quad (16)$$

where $C_{m\&m}$is a coefficient equal to 0.004786 [m$^{0.33}$ s$^{-0.22}$], $r_p$is the radius of the liquid pool [m], $u_{w,10}$ is the wind speed at standard 10-metre height [m s^{-1}], and Sc is the Schmidt number [-]. Generally, for gases and vapours, the Schmidt number (Sc) is approximately equal to 0.8. To calculate c_i, the Antoine equation was used.

Dispersion modelling

To simulate the dispersion of pollutants in the atmosphere, the Parallel Micro-Swift Spray (PMSS) code, developed by Arianet, was used (Oldrini et al., 2017). Parallel Micro-Swift Spray is a micro-scale modelling system based on the use of three-dimensional Lagrangian particle modelling for the simulation of the transport and dispersion of pollutants with the possibility of conducting simulations in generally shorter time frames than those required by more complex Computational Fluid Dynamics models (Oldrini & Armand, 2019). The system consists

Downloaded from https://academic.oup.com/ieam/advance-article/doi/10.1093/inteam/vjaf073/8164122 by guest on 27 June 2025

of PSwift, a diagnostic meteorological pre-processor based on the principle of minimizing the divergence of the velocity field, which includes semi-empirical parameterizations to reproduce the effects of wakes and recirculation induced by the presence of buildings. It also includes the parallel and micro-scale Spray Lagrangian particle dispersion model. The code is parallelizable, meaning it can perform operations in parallel on computers or computer networks in a distributed memory configuration using the MPI protocol (Oldrini et al., 2017).

In the case study, the spatial domain considered for the analysis of dispersion consisted of a grid of 560 x 450 m, with cells of 2-m sides (281 x 226 points). This horizontal resolution was chosen to obtain a good representation of the built elements present at the site. Weather data provided by a meteorological monitoring station located 6 km west of the industrial site, with hourly resolution, were used. Meteorological data included the following parameters: wind speed and direction, solar radiation, temperature, atmospheric pressure, and precipitation. Meteorological data were pre-processed with PSwift and Surfpro models to obtain wind fields and dispersion parameters. The presence and shape of building elements were also introduced in PSwift to assess the perturbation to the flow (wake and recirculation effects) caused by their presence. As meteorological data from the year 2002 were not available, data from 2021 were used. However, the most critical dispersion conditions were considered, analysing ambient temperature and the Monin-Obukhov length. A period including low ambient temperature (limited convection) and both stable and unstable atmospheric conditions (positive and negative values of L_M) was selected, and dispersion was simulated based on such conditions.

Short-term risk calculation

In the present study, only the short-term inhalation risk was considered, given the rapid dynamics of the release event. Indeed, it is unlikely that such an event would result in

Downloaded from https://academic.oup.com/ieam/advance-article/doi/10.1093/inteam/vjaf073/8164122 by guest on 27 June 2025

368 prolonged exposure to the toxic substance, as the plant would be evacuated. The risk is
369 therefore assumed to be solely related to short-term exposures due, for example, to the
370 period prior to evacuation or the activity of emergency response personnel.

371 Short-term inhalation risk was calculated using the mean of Equation 1. The exposure factor
372 EF was assumed equal to unity, assuming the constant presence of workers who intervened
373 to mitigate the incident. To evaluate the short-term inhalation risk, concentration fields were
374 compared to the threshold limit values proposed by the ACGIH. The TLV-STEL (Threshold Limit
375 Value - Short Term Exposure Limit) was considered (American Conference of Governmental
376 Industrial Hygienists, 2024). The TLV-STEL is the limit for short exposures, representing the
377 average concentration that can be tolerated for a maximum of 15 minutes, no more than four
378 times a day, with at least one hour between exposure periods. The recommended TLV-STEL
379 for tetrahydrofuran is 100 ppm (295 mg m^{-3}). In dispersion modelling, concentration averaging
380 depends on the time resolution of meteorological input, which for this scale of analysis is
381 usually hourly. For this, concentration values must be corrected to take into account the
382 possibility that a shorter-period (15 minutes) mean could be higher than a 1-hour mean. In
383 the specific case, 15-minute mean concentrations were calculated with Equation 2. A value of
384 0.3 was assigned to the exponent n, resulting in a multiplying factor of 1.52. According to
385 Bartzis et al. (2008), n=0.3 is reasonable based on past experience. Thus, for risk calculation,
386 1-hour mean concentration fields were multiplied by a factor of 1.52. It must be noted that
387 Equation 2 presents inconsistencies when $\Delta\tau$ becomes very large and thus $\overline{C}(\Delta\tau)$ tends to
388 zero, and hence corrections need to be applied according to Bartzis et al. (2008). However, in
389 this specific case, $\Delta\tau$ is limited; thus this relation can be applied without corrections.

390 **RESULTS**

Downloaded from https://academic.oup.com/ieam/advance-article/doi/10.1093/inteam/vjaf073/8164122 by guest on 27 June 2025

The accidental event consisted in the failure of a storage vessel containing tetrahydrofuran, and the consequent release of the substance. From the onset of liquid release, a pool formed in the containment basin. Some of the liquid continued to spill from the tank into the containment basin, while a portion of that already in the basin began to evaporate. The pool volume initially increased, as the tank release rate exceeded the rate of evaporation. After the complete emptying of the tank, the liquid kept evaporating from the pool. Complete pool evaporation occurred within approximately 24 hours. The evaporation rate was subject to variations depending on environmental conditions, such as wind speed and atmospheric temperature. The whole event included periods of both stable and unstable atmospheric conditions. The mass flow of tetrahydrofuran released from the vessel, and the evaporation rate, are reported in Figure 3.

From the simulations conducted using the pre-processors PSWIFT and SURFPRO, hourly wind fields and turbulence parameters were obtained. These data were generated taking into account the configuration of buildings in the area under consideration. Wind fields at two hours into the event, corresponding to stable and unstable atmospheric conditions, are represented in Figure A.1 (Supporting information). Induced disturbance of constructed elements to the airflow is clearly visible. Under stable atmospheric conditions, the prevailing wind direction is NE. Wind speed is low, and some areas of stagnation can be seen in the areas most heavily surrounded by built elements. At the same time, restrictions between buildings cause a local increase of air speed. In unstable atmospheric conditions, the prevailing wind direction is SW and wind speed is higher. The direction of the flow changes only in areas mostly enclosed by buildings. The wake effect of built elements is also clearly visible.

Two maps of the hourly mean concentration of tetrahydrofuran, one for stable and one for unstable atmospheric conditions, referring to a height of 2 metres above the ground, were

Downloaded from https://academic.oup.com/ieam/advance-article/doi/10.1093/inteam/vjaf073/8164122 by guest on 27 June 2025

generated (Figure 4). As reported in the previous section, 1-hour concentration fields were multiplied by a factor of 1.52 to apply a correction for the duration of short-term exposure (15 minutes). Figure 4 shows that the tetrahydrofuran concentration within the appurtenances of the industrial area is between 0 and 596 mg m^{-3} for both stable and unstable conditions. The concentration decreases rapidly with distance from the source. The direction of the plume is strictly correlated with the main wind. Also, areas of pollutant accumulation are visible near the buildings, caused by recirculation phenomena occurring in the air flow field. As expected, the mean concentration is higher during stable conditions.

Vertical profiles of tetrahydrofuran concentration, in correspondence with two points close to the emission source, are reported in Figure 5. Figure 5 shows that concentrations peak at the source height, then decrease exponentially to a negligible value at around 12 - 14 metres. At point A (downwind in stable atmospheric conditions) concentrations are higher than at point B (downwind in unstable atmospheric conditions), probably due to different wind speeds. Between 2 and 4 metres of height, concentrations are higher in the case of stable atmospheric conditions, while between 4 and 9 metres they are higher in the case of unstable conditions. At point B, concentrations are always higher in the case of stable concentrations.

Maps of inhalation risk for stable and unstable conditions are reported in Figure 6. It is recalled that the TLV-STEL is the limit for short exposures, representing the average concentration that can be tolerated for a maximum of 15 minutes, no more than four times a day, with at least one hour between exposure periods. For tetrahydrofuran, this limit is set at 100 ppm (American Conference of Governmental Industrial Hygienists, 2024). Also, the standard criteria for non-carcinogenic risk assessment provide that risk is acceptable when the HQ value is less than one.

Downloaded from https://academic.oup.com/ieam/advance-article/doi/10.1093/inteam/vjaf073/8164122 by guest on 27 June 2025

The results show that the inhalation risk is negligible from around 10 metres distance from the source. However, the limit of HQ>1 is exceeded frequently during the event. A map of the limit exceedances is reported in Figure 7. This figure shows the spatial distribution and frequency of risk exceedances during the entire event. Risk limit is exceeded as much as 21 times, but only in correspondence with the release area. Absolute maximum concentration is reached in the first hour of the event and is 596 mg m^{-3}. At every time step of the simulation, maximum concentration is detected inside the perimeter of the source. In the remainder of the area, concentration quickly decreases with distance from the source, and the HQ is below unity.

DISCUSSION

In the specific case study, the results show that the accidental event triggered by a NaTech does not generate a relevant risk for the inhalation of tetrahydrofuran, despite the TLV-STEL's being exceeded at certain times in correspondence with the source. The case study presented is intended to be a means of showing the applicability of the general methodology. The variables involved are many and could have a significant effect on the potential risk to workers. For the same geometric and topographical configuration of the site, the characteristics of a released substance (especially density and volatility) could greatly influence the duration and effects of the release. Less volatile substances would evaporate more slowly, resulting in less transport to the atmospheric compartment. For example, if under the same conditions the released substance had been methyl ethyl ketone (ρ=805 kg m^{-3}; TLV-STEL=150 ppm), the pool evaporation of the substance would have lasted 46 hours. If, on the other hand, it had been ethylbenzene (ρ=866 kg m^{-3}; TLV-STEL=200 ppm), the evaporation of the puddle would have lasted as long as 34 days, presumably allowing intervention for the containment of the release prior to evaporation. Similar considerations

Downloaded from https://academic.oup.com/ieam/advance-article/doi/10.1093/inteam/vjaf073/8164122 by guest on 27 June 2025

can be made for the type of release (Qingchun & Laibin, 2011) taking into account that, as reported by Jain et al. (2017), the dynamics of an accident could be extremely complex and difficult to predict. The integration of a model for dynamic risk analysis, as suggested by Paltrinieri and Reniers (2017), might also be appropriate.

The adoption of different reference databases for exposure limits may also have a significant influence on the final result. In the present case, two different short-term exposure limit values were reported, one twice as high as the other. Had the less restrictive one (250 ppm or 735 mg m^{-3} proposed by NIOSH) been applied, the number of exceedances would have decreased to zero. Similarly, discussion is still open in the scientific community on the most appropriate approach to follow for correcting average concentration values over short time periods. In particular, there is a need to choose approaches for calculating peak-to-mean that are sufficiently rigorous but relatively simple to apply in terms of time and data availability (Brancher et al., 2020).

With regard to the proposed general methodology, it is necessary to work on subsequent refinements in order to, at the same time, ensure sufficiently general applicability and reduce the uncertainties associated with each individual operational step. This approach is followed at present, particularly for large-scale major accidents, i.e. involving spatial scales on the order of several km (Benamrane et al., 2013). For example, the Accident Damage Assessment Module (ADAM), developed by the Joint Research Centre of the European Commission (European Commission. Joint Research Centre., 2017), and the BenMap-CE tool (Malakan et al., 2024), are two of the most consolidated models that can be applied at this scope. On the other hand, for micro-scale accidents in the working environment, a comprehensive and general methodology still needs further development. In this context, the present work

Downloaded from https://academic.oup.com/ieam/advance-article/doi/10.1093/inteam/vjaf073/8164122 by guest on 27 June 2025

suggests a model that can be applied with relatively low costs in terms of data and calculation time.

In the present study, the simulation of the dispersion during the entire event took approximately 1.5 hours on a 48-core parallel scheduler (1 GB/core). Even though the computational time of the PMSS model has been observed to be significantly lower than CFD models, the need to simulate the accident and intervene in a short time requires that the computational time be further reduced.

Finally, the prediction of possible side effects at the microscale due to NaTech events must be more closely integrated into the QRA (quantitative risk analysis) procedures applied to industrial processes, both within the scope of the Seveso III directive (Necci et al., 2015) and for non-Seveso plants, such as small and medium enterprises, that can be potentially affected by accidents (Gajek and Michalik, 2013).

CONCLUSIONS

The proposed methodology has significant implications for emergency management in industrial settings. By providing rapid and high-resolution inhalation risk assessments, the methodology can support decision-making before the occurrence of NaTech events, enabling more effective protective measures for workers. Industrial facilities can use the methodology for scenario planning and training, improving preparedness for potential NaTech events. The presented model can be applied with relatively limited resources in terms of data and calculation time. It combines precision, timeliness, and practical applicability. The application of a Lagrangian particle model capable of simulating the presence of buildings in the dispersion area allows a detailed screening of the possible dispersion pathways under varying meteorological conditions, with lower computational effort and comparable precision,

Downloaded from https://academic.oup.com/ieam/advance-article/doi/10.1093/inteam/vjaf073/8164122 by guest on 27 June 2025

compared to computational fluid dynamics. The general approach needs to be tested extensively and integrated with analysis of NaTech event dynamics and existing consolidated methodologies for quantitative risk analysis. With further development and validation, this methodology could become an important tool for health protection in industrial sites, faced with the many challenges of climate change. Continued research and technological advancements in this field will be essential for improving our preparedness and response to the complex effects posed by NaTech events. Future research should focus on improving model integration and reducing uncertainties. Moreover, there is a need for interdisciplinary collaboration to enhance the applicability of these models across different industrial sectors and geographical regions.

Downloaded from https://academic.oup.com/ieam/advance-article/doi/10.1093/inteam/vjaf073/8164122 by guest on 27 June 2025

519

520 **FIGURE CAPTIONS**

521 Figure 1. Methodology workflow

522 Figure 2. Plan view of the industrial settlement

523 Figure 3. Tetrahydrofuran cumulated spill and evaporation during the release event. Air
524 temperature and wind speed are also reported. For better graphic visualization, wind speed
525 observations are multiplied by a factor of 10.

526 Figure 4. 15-minute mean tetrahydrofuran corrected concentration during a) stable
527 atmospheric conditions, and b) unstable atmospheric conditions. This concentration map was
528 obtained by multiplying 1-hour mean modelled concentration by a factor of 1.52. Different
529 meteorological and atmospheric conditions significantly affect plume direction and horizontal
530 spread.

531 Figure 5. Vertical profiles of tetrahydrofuran concentration in two arbitrarily selected
532 locations close to the emission source. The positions of receptors A and B are reported in the
533 figure onset. Concentration module decreases rapidly with height.

534 Figure 6. Short-term inhalation hazard quotient map in a) stable, and b) unstable atmospheric
535 conditions. Hazard quotient approaches unity (red colour, indicating non-negligible risk) only
536 in close proximity to the release source.

537 Figure 7. Position and frequency of exceedances of the threshold limit value during the entire
538 event. Numbers indicate the times (number of hours) the limit was exceeded during the entire
539 event, which lasted 25 hours.

540

Downloaded from https://academic.oup.com/ieam/advance-article/doi/10.1093/inteam/vjaf073/8164122 by guest on 27 June 2025

541 **TABLE CAPTIONS**

542 Table 1. Properties of tetrahydrofuran (Dannan, 2015)

543

Downloaded from https://academic.oup.com/ieam/advance-article/doi/10.1093/inteam/vjaf073/8164122 by guest on 27 June 2025

544 **REFERENCES**

545 American Conference of Governmental Industrial Hygienists (ACGIH). (2024).
546 https://www.acgih.org/
547 Bartzis, J. G., Sfetsos, A., & Andronopoulos, S. (2008). On the individual exposure from
548 airborne hazardous releases: The effect of atmospheric turbulence. *Journal of*
549 *Hazardous Materials*, *150*(1), 76–82. https://doi.org/10.1016/j.jhazmat.2007.04.078
550 Benamrane, Y., Wybo, J.-L., & Armand, P. (2013). Chernobyl and Fukushima nuclear
551 accidents: What has changed in the use of atmospheric dispersion modeling?
552 *Journal of Environmental Radioactivity*, *126*, 239–252.
553 https://doi.org/10.1016/j.jenvrad.2013.07.009
554 Berchet, A., Zink, K., Muller, C., Oettl, D., Brunner, J., Emmenegger, L., & Brunner, D. (2017).
555 A cost-effective method for simulating city-wide air flow and pollutant dispersion at
556 building resolving scale. *Atmospheric Environment*, *158*, 181–196.
557 https://doi.org/10.1016/j.atmosenv.2017.03.030
558 Blocken, B., Stathopoulos, T., Saathoff, P., & Wang, X. (2008). Numerical evaluation of
559 pollutant dispersion in the built environment: Comparisons between models and
560 experiments. *Journal of Wind Engineering and Industrial Aerodynamics*, *96*(10–11),
561 1817–1831. https://doi.org/10.1016/j.jweia.2008.02.049
562 Brancher, M., Hieden, A., Baumann-Stanzer, K., Schauberger, G., & Piringer, M. (2020).
563 Performance evaluation of approaches to predict sub-hourly peak odour
564 concentrations. *Atmospheric Environment: X*, *7*, 100076.
565 https://doi.org/10.1016/j.aeaoa.2020.100076
566 Cangmin, L., & Klauk, A. (2020). *Sino-German Chemicals Management Joint Research Project*
567 *Report*. Foreign Environmental Cooperation Center, Ministry of Ecology and

Downloaded from https://academic.oup.com/ieam/advance-article/doi/10.1093/inteam/vjaf073/8164122 by guest on 27 June 2025

Environment, FECO; Deutsche Gesellschaft für Internationale Zusammenarbeit, GIZ. https://www.international-climate-initiative.com/fileadmin/iki/Dokumente/Publikationen/Projekte/17_I_329/1_Sino-German_Chemicals_Management_-_Joint_Research_Project_Report.pdf

Carini, A., Cecchi, S., & Orcioni, S. (2018). Orthogonal LIP Nonlinear Filters. In *Adaptive Learning Methods for Nonlinear System Modeling* (pp. 15–46). Elsevier. https://doi.org/10.1016/B978-0-12-812976-0.00003-8

Cruz, A. M., & Suarez-Paba, M. C. (2019). Advances in Natech research: An overview. *Progress in Disaster Science*, *1*, 100013. https://doi.org/10.1016/j.pdisas.2019.100013

Dannan, G. A. (2015). Tetrahydrofuran. In R. D. Harbison, M. M. Bourgeois, & G. T. Johnson (A c. Di), *Hamilton & Hardy's Industrial Toxicology* (pp. 719–726). John Wiley & Sons, Inc. https://doi.org/10.1002/9781118834015.ch70

Dou, Z., Liu, Z., Li, L., Zhou, H., Wang, Q., Zhang, J., & Chen, L. (2022). Atmospheric dispersion prediction of accidental release: A review. *Emergency Management Science and Technology*, *2*(1), 1–20. https://doi.org/10.48130/EMST-2022-0009

European Commission. (2024a). *Health and safety at work—Scientific Committee on Occupational Exposure Limits*. https://ec.europa.eu/social/main.jsp?catId=148&langId=en&intPageId=684

European Commission. (2024b). *The Major Accident Reporting System (eMARS)*. https://emars.jrc.ec.europa.eu/en/emars/content

European Commission. Joint Research Centre. (2017). *Accident Damage Analysis Module (ADAM): Technical guidance : software tool for consequence analysis calculations.* Publications Office. https://data.europa.eu/doi/10.2760/719457

Downloaded from https://academic.oup.com/ieam/advance-article/doi/10.1093/inteam/vjaf073/8164122 by guest on 27 June 2025

Fabbri, L., & Wood, M. H. (2019). Accident Damage Analysis Module (ADAM): Novel European Commission tool for consequence assessment—Scientific evaluation of performance. *Process Safety and Environmental Protection*, *129*, 249–263. https://doi.org/10.1016/j.psep.2019.07.007

Fleming, P., Annoni, J., Shah, J. J., Wang, L., Ananthan, S., Zhang, Z., Hutchings, K., Wang, P., Chen, W., & Chen, L. (2017). Field test of wake steering at an offshore wind farm. *Wind Energy Science*, *2*(1), 229–239. https://doi.org/10.5194/wes-2-229-2017

Gajek, A. & Michalik, J. (2013). Major accident hazard posed by non-seveso establishments in poland and management in the area of their control. *Chemical Engineering Transactions*, *31*, 169–174. https://doi.org/10.3303/CET1331029

Gowardhan, A. A., Pardyjak, E. R., Senocak, I., & Brown, M. J. (2011). A CFD-based wind solver for an urban fast response transport and dispersion model. *Environmental Fluid Mechanics*, *11*(5), 439–464. https://doi.org/10.1007/s10652-011-9211-6

Grašič, B., Mlakar, P., Božnar, M. Z., & Kocijan, J. (2018). Validation of numerically forecast vertical temperature profile with measurements for dispersion modelling. *International Journal of Environment and Pollution*, *64*(1/2/3), 22. https://doi.org/10.1504/IJEP.2018.099143

Hassan Bhat, T., Jiawen, G., & Farzaneh, H. (2021). Air Pollution Health Risk Assessment (AP-HRA), Principles and Applications. *International Journal of Environmental Research and Public Health*, *18*(4), 1935. https://doi.org/10.3390/ijerph18041935

Houf, W. G., & Winters, W. S. (2013). Simulation of high-pressure liquid hydrogen releases. *International Journal of Hydrogen Energy*, *38*(19), 8092–8099. https://doi.org/10.1016/j.ijhydene.2013.01.052

Downloaded from https://academic.oup.com/ieam/advance-article/doi/10.1093/inteam/vjaf073/8164122 by guest on 27 June 2025

Jain, P., Pasman, H. J., Waldram, S. P., Rogers, W. J., & Mannan, M. S. (2017). Did we learn about risk control since Seveso? Yes, we surely did, but is it enough? An historical brief and problem analysis. *Journal of Loss Prevention in the Process Industries*, *49*, 5–17. https://doi.org/10.1016/j.jlp.2016.09.023

Jones, A. R., Leadbetter, S. J., & Hort, M. C. (2023). Using synthetic case studies to explore the spread and calibration of ensemble atmospheric dispersion forecasts. *Atmospheric Chemistry and Physics*, *23*(19), 12477–12503. https://doi.org/10.5194/acp-23-12477-2023

Karaca, F., Kumisbek, A., Inglezakis, V. J., Azat, S., Zhakiyenova, A., Ormanova, G., & Guney, M. (2021). DIMIZA: A dispersion modeling based impact zone assessment of mercury (Hg) emissions from coal-fired power plants and risk evaluation for inhalation exposure. *Engineering Reports*, *3*(7), e12357. https://doi.org/10.1002/eng2.12357

Kawamura, P. I., & Mackay, D. (1987). The evaporation of volatile liquids. *Journal of Hazardous Materials*, *15*(3), 343–364. https://doi.org/10.1016/0304-3894(87)85034-3

Kocijan, J., Hvala, N., Perne, M., Mlakar, P., Grašič, B., & Božnar, M. Z. (2023). Surrogate modelling for the forecast of Seveso-type atmospheric pollutant dispersion. *Stochastic Environmental Research and Risk Assessment*, *37*(1), 275–290. https://doi.org/10.1007/s00477-022-02288-x

Koopman, R. P., & Ermak, D. L. (2007). Lessons learned from LNG safety research. *Journal of Hazardous Materials*, *140*(3), 412–428. https://doi.org/10.1016/j.jhazmat.2006.10.042

Downloaded from https://academic.oup.com/ieam/advance-article/doi/10.1093/inteam/vjaf073/8164122 by guest on 27 June 2025

Krausmann, E., Cruz, A. M., & Salzano, E. (2017). *Natech risk assessment and management: Reducing the risk of natural-hazard impact on hazardous installations*. Elsevier.

Maidment, S. (1998). Occupational hygiene considerations in the development of a structured approach to select chemical control strategies. *The Annals of Occupational Hygiene*, *42*(6), 391–400. https://doi.org/10.1016/S0003-4878(98)00049-0

Malakan, W., Thepanondh, S., Keawboonchu, J., Kultan, V., Kondo, A., & Shimadera, H. (2024). Integrated assessment of inhalation health risk and economic benefit of improving ambient targeted VOCs in Petrochemical industrial area. *Air Quality, Atmosphere & Health*. https://doi.org/10.1007/s11869-024-01552-z

Markiewicz, M. (2012). A Review of Mathematical Models for the Atmospheric Dispersion of Heavy Gases. Part I. A Classification of Models. *Ecological Chemistry and Engineering S*, *19*(3), 297–314. https://doi.org/10.2478/v10216-011-0022-y

Mathworks Inc. (2024). *Matlab R2023b*. https://mathworks.com/

Melo, A. L. V., Santos, J. M., Reis, N. C., Castro, I. P., V Goulart, E., & Xie, Z. T. (2023). Influence of wind direction and source location on peak-to-mean concentration ratios in urban environments. *Journal of Wind Engineering and Industrial Aerodynamics*, *232*, 105264. https://doi.org/10.1016/j.jweia.2022.105264

Monin, A. S., & Obukhov, A. M. (s.d.). Basic laws of turbulent mixing in the surface layer of the atmosphere. *Tr. Akad., Nauk SSSR Geophiz. Inst., 24*, 30.

National Institute for Health (NIH), 1994. Approaches for estimating the distribution of short-term exposure concentrations for different averaging time. The Annals of Occupational Hygiene. https://doi.org/10.1093/annhyg/38.6.815

Downloaded from https://academic.oup.com/ieam/advance-article/doi/10.1093/inteam/vjaf073/8164122 by guest on 27 June 2025

National Institute for Occupational Safety and Health. (2024). https://www.cdc.gov/niosh/index.html

Necci, A., Cozzani, V., Spadoni, G., & Khan, F. (2015). Assessment of domino effect: State of the art and research Needs. *Reliability Engineering & System Safety*, *143*, 3–18. https://doi.org/10.1016/j.ress.2015.05.017

Occupational Safety and Health Administration. (2024). https://www.osha.gov/

Oldrini, O., & Armand, P. (2019). Validation and Sensitivity Study of the PMSS Modelling System for Puff Releases in the Joint Urban 2003 Field Experiment. *Boundary-Layer Meteorology*, *171*(3), 513–535. https://doi.org/10.1007/s10546-018-00424-1

Oldrini, O., Armand, P., Duchenne, C., Olry, C., Moussafir, J., & Tinarelli, G. (2017). Description and preliminary validation of the PMSS fast response parallel atmospheric flow and dispersion solver in complex built-up areas. *Environmental Fluid Mechanics*, *17*(5), 997–1014. https://doi.org/10.1007/s10652-017-9532-1

Pal, A., Ul Karim, I., Mondal, B., & Raha, S. (2018). A Similarity Based Fuzzy System as a Function Approximator. *International Journal of Intelligence Science*, *08*(04), 89–116. https://doi.org/10.4236/ijis.2018.84005

Paltrinieri, N., & Reniers, G. (2017). Dynamic risk analysis for Seveso sites. *Journal of Loss Prevention in the Process Industries*, *49*, 111–119. https://doi.org/10.1016/j.jlp.2017.03.023

Perne, M., Božnar, M. Z., Grašič, B., Mlakar, P., & Kocijan, J. (2021). Improving wind vector predictions for modelling of atmospheric dispersion during Seveso-type accidents. *Atmospheric Pollution Research*, *12*(2), 76–83. https://doi.org/10.1016/j.apr.2020.10.010

Downloaded from https://academic.oup.com/ieam/advance-article/doi/10.1093/inteam/vjaf073/8164122 by guest on 27 June 2025

Qingchun, M., & Laibin, Z. (2011). CFD simulation study on gas dispersion for risk assessment: A case study of sour gas well blowout. *Safety Science*, *49*(8–9), 1289–1295. https://doi.org/10.1016/j.ssci.2011.04.016

Rademaeker, E. D. & Associazione Italiana di Ingegneria Chimica (A c. Di). (2012). *CISAP5, 5th International Conference on Safety & Environment in Process & Power Industry: 3 - 6 June 2012, Milan, Italy*. AIDIC.

Ravina, M., Bruzzese, S., Panepinto, D., & Zanetti, M. (2020). Analysis of Separation Distances under Varying Odour Emission Rates and Meteorology: A WWTP Case Study. *Atmosphere*, *11*(9), 962. https://doi.org/10.3390/atmos11090962

Ravina, M., Facelli, A., & Zanetti, M. (2020). Halocarbon Emissions from Hazardous Waste Landfills: Analysis of Sources and Risks. *Atmosphere*, *11*(4), 375. https://doi.org/10.3390/atmos11040375

SafeWork Australia. (2024). https://www.safeworkaustralia.gov.au/

Shafiei Moghaddam, P., Jahangiri, K., Sohrabizadeh, S., Hassani, N., Hoseini Moghaddam, M., & Tehrani, G. M. (2023). Foresight of the Consequences of the Hazmat Release From an Oil Refinery on the Surrounding Urban Community Following an Earthquake: A Natech Scenario Analysis. *Disaster Medicine and Public Health Preparedness*, *17*, e79. https://doi.org/10.1017/dmp.2021.349

Teggi, S., Costanzini, S., Ghermandi, G., Malagoli, C., & Vinceti, M. (2018). A GIS-based atmospheric dispersion model for pollutants emitted by complex source areas. *Science of The Total Environment*, *610–611*, 175–190. https://doi.org/10.1016/j.scitotenv.2017.07.196

Downloaded from https://academic.oup.com/ieam/advance-article/doi/10.1093/inteam/vjaf073/8164122 by guest on 27 June 2025

Torrontegui, E., & García-Ripoll, J. J. (2019). Unitary quantum perceptron as efficient universal approximator. *EPL (Europhysics Letters)*, *125*(3), 30004. https://doi.org/10.1209/0295-5075/125/30004

Trini Castelli, S., Armand, P., Tinarelli, G., Duchenne, C., & Nibart, M. (2018). Validation of a Lagrangian particle dispersion model with wind tunnel and field experiments in urban environment. *Atmospheric Environment*, *193*, 273–289. https://doi.org/10.1016/j.atmosenv.2018.08.045

United Kingdom Government. (2024). *Control of substances hazardous to health (COSHH)*. https://www.hse.gov.uk/cleaning/topics/coshh.htm#:~:text=you%20must%20do-,Control%20of%20Substances%20Hazardous%20to%20Health%20(COSHH)%20Regulations%202002%20(,those%20resulting%20from%20serious%20spillages.

U.S. Environmental Protection Agency. (2024). *Risk Assessment Guidance for Superfund: Volume I Human Health Evaluation Manual (Part F, Supplemental Guidance for Inhalation Risk Assessment)*. https://www.epa.gov/risk/risk-assessment-guidance-superfund-rags-part-f

van den Bosch, C. J. H., & R.A.P.M. Weterings. (2005). *Methods for the calculation of physical effects due to releases of hazardous materials (liquid and gases)*. https://publications.tno.nl/publication/34634119/QIKv78/TNO-2005-yellow.pdf

Zhang, X., & Wang, J. (2022). Atmospheric dispersion of chemical, biological, and radiological hazardous pollutants: Informing risk assessment for public safety. *Journal of Safety Science and Resilience*, *3*(4), 372–397. https://doi.org/10.1016/j.jnlssr.2022.09.001

Downloaded from https://academic.oup.com/ieam/advance-article/doi/10.1093/inteam/vjaf073/8164122 by guest on 27 June 2025

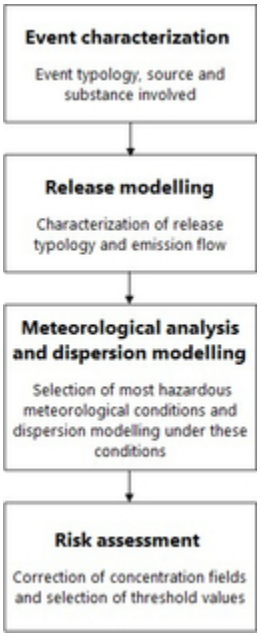

Figure 1. Methodology workflow.

10x26mm (300 x 300 DPI)

Downloaded from https://academic.oup.com/ieam/advance-article/doi/10.1093/inteam/vjaf073/8164122 by guest on 27 June 2025

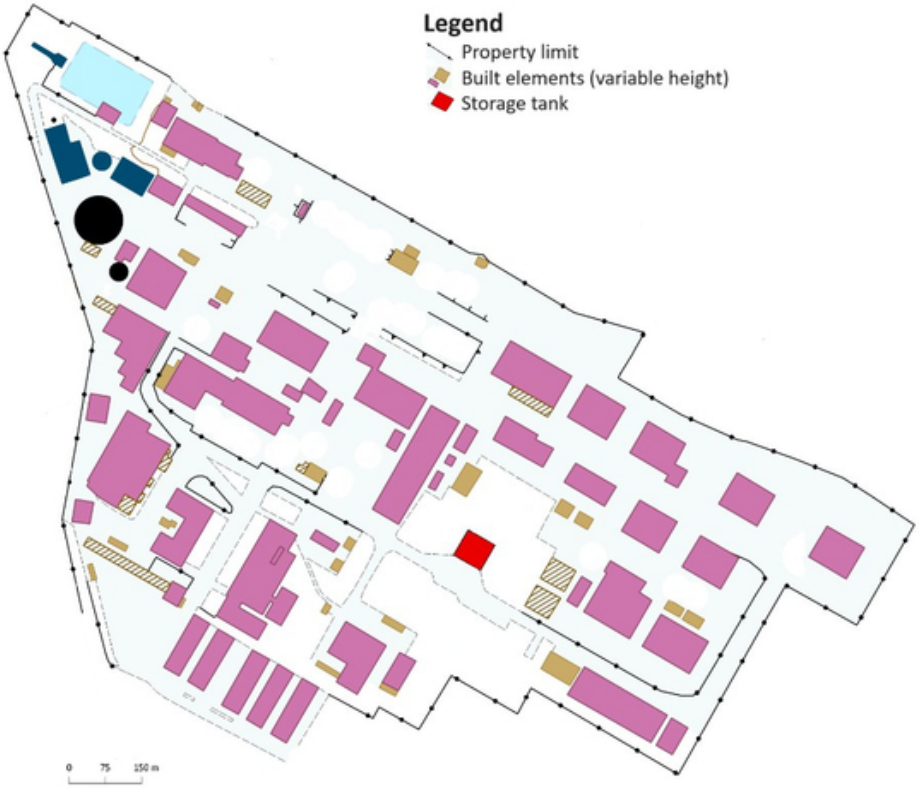

Figure 2. Plan view of the industrial settlement.

49x40mm (300 x 300 DPI)

Downloaded from https://academic.oup.com/ieam/advance-article/doi/10.1093/inteam/vjaf073/8164122 by guest on 27 June 2025

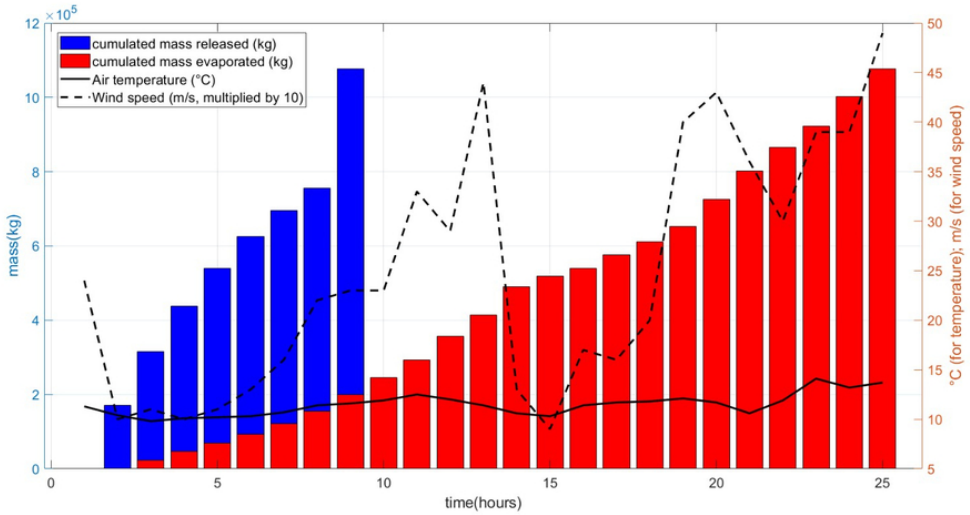

Figure 3. Tetrahydrofuran cumulated spill and evaporation during the release event. Air temperature and wind speed are also reported. For better graphic visualization, wind speed observation are multiplied by a factor of 10.

76x39mm (300 x 300 DPI)

Downloaded from https://academic.oup.com/ieam/advance-article/doi/10.1093/inteam/vjaf073/8164122 by guest on 27 June 2025

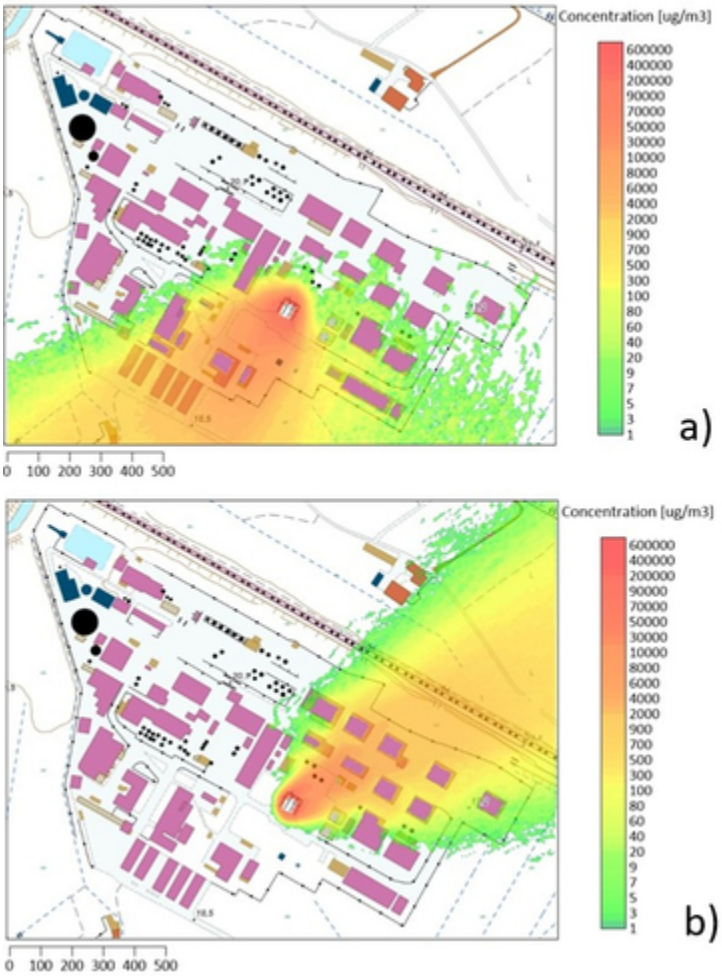

Figure 4. 15-minutes mean tetrahydrofuran corrected concentration during a) stable atmospheric conditions, and b) unstable atmospheric conditions. This concentration map was obtained by multiplying 1-hour mean modelled concentration by a factor of 1.52. Different meteorological and atmospheric conditions affect significantly plume direction and horizontal spread.

30x42mm (300 x 300 DPI)

Downloaded from https://academic.oup.com/ieam/advance-article/doi/10.1093/inteam/vjaf073/8164122 by guest on 27 June 2025

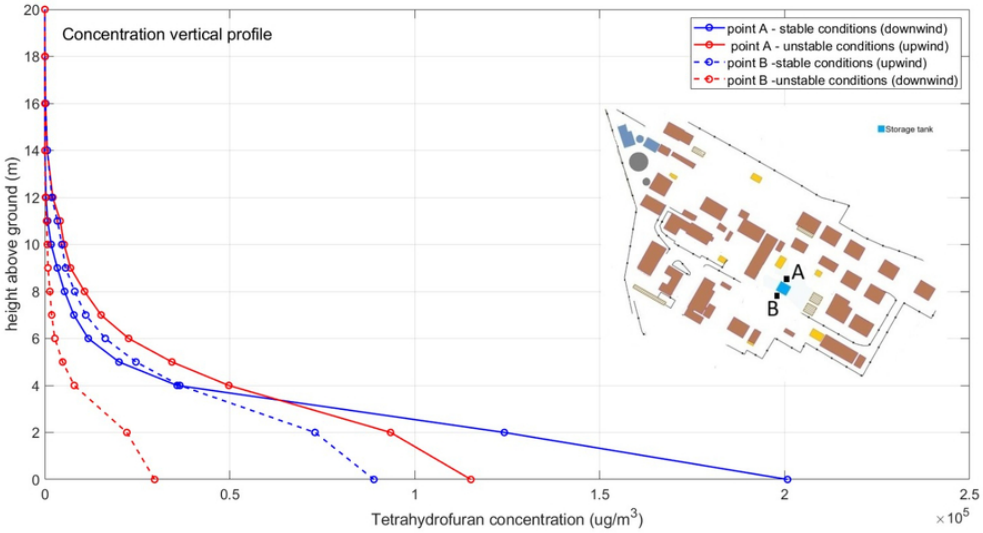

Figure 5. Vertical profiles of tetrahydrofuran concentration in two arbitrarily selected position close to the emission source. The position of receptors A and B is reported in the figure onset. Concentration module decreases rapidly with height.

76x41mm (300 x 300 DPI)

Downloaded from https://academic.oup.com/ieam/advance-article/doi/10.1093/inteam/vjaf073/8164122 by guest on 27 June 2025

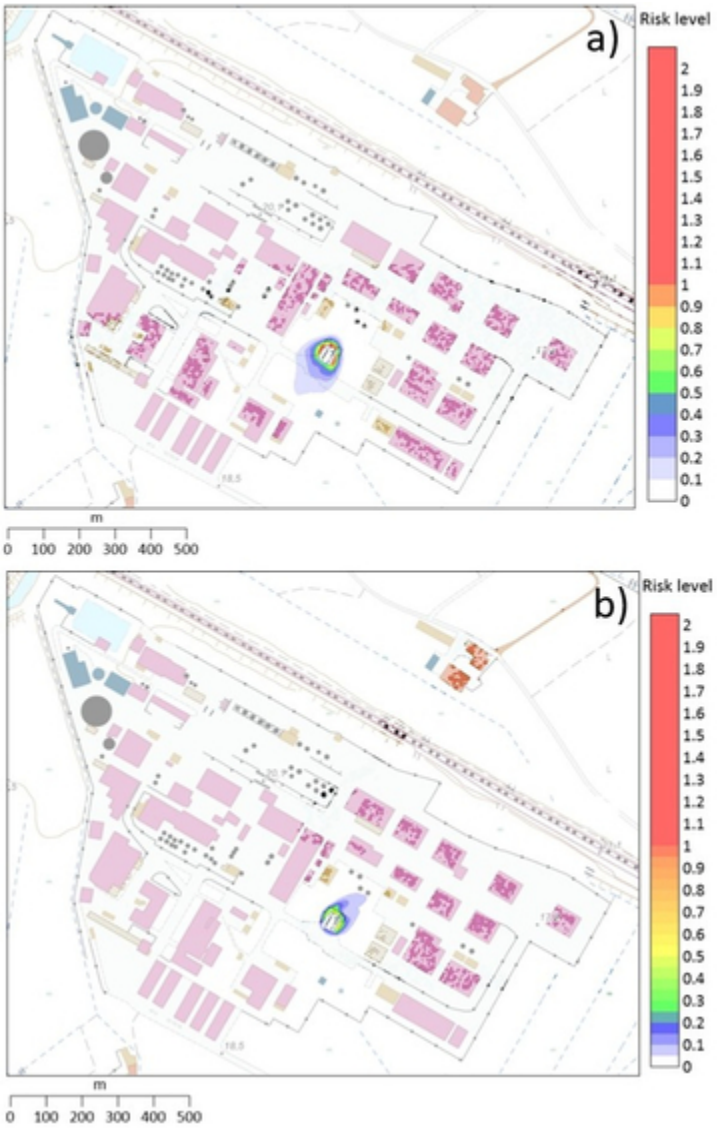

Figure 6. Short-term inhalation hazard quotient map in a) stable, and b) unstable atmospheric conditions. Hazard quotient approaches unity (red color, indicating non-negligible risk) only in close proximity of the release source.

30x48mm (300 x 300 DPI)

Downloaded from https://academic.oup.com/ieam/advance-article/doi/10.1093/inteam/vjaf073/8164122 by guest on 27 June 2025

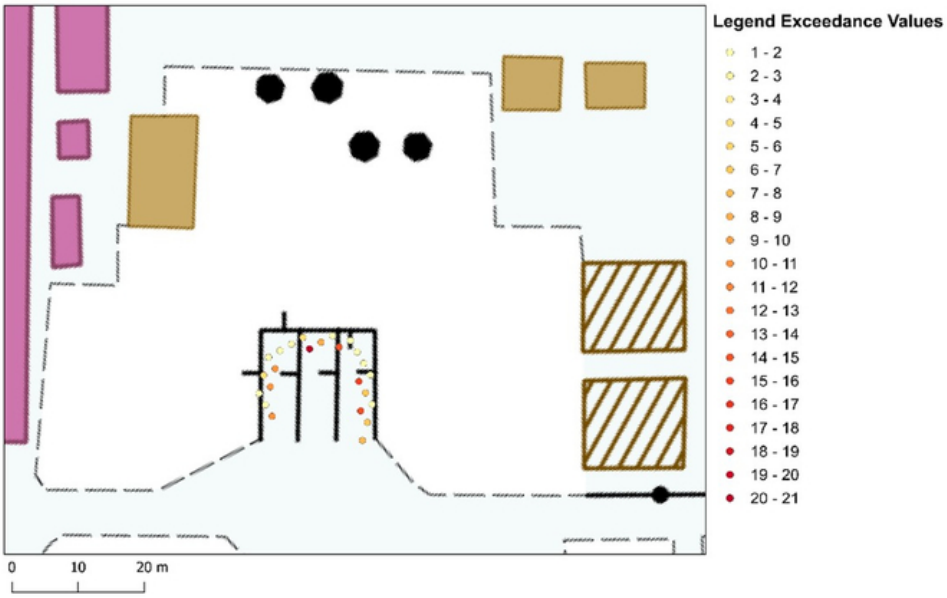

Figure 7. Position and frequency of exceedances of the threshold limit value during the whole event. Numbers indicate the times (number of hours) the limit was exceeded during the entire event, that lasted 25 hours.

58x35mm (300 x 300 DPI)

Downloaded from https://academic.oup.com/ieam/advance-article/doi/10.1093/inteam/vjaf073/8164122 by guest on 27 June 2025

Formula	C_4H_8O
Molecular weight (g mol^{-1})	72.1057
CAS number	109-99-9
Density at 25°C (g ml^{-1})	0.881
Henry's law constant for solubility in water at 25°C (mol kg^{-1} bar^{-1})	14
TLV-STEL (ppm)	100
NIOSH REL (ppm)	250

Downloaded from https://academic.oup.com/ieam/advance-article/doi/10.1093/inteam/vjaf073/8164122 by guest on 27 June 2025